

Fast Layout-Oblivious Tensor-Matrix Multiplication with BLAS

Cem Savaş Başsoy

Hamburg University of Technology, Schwarzenbergstrasse 95, Germany,
cem.bassoy@gmail.com

Abstract. The tensor-matrix multiplication is a basic tensor operation required by various tensor methods such as the ALS and the HOSVD. This paper presents flexible high-performance algorithms that compute the tensor-matrix product according to the Loops-over-GEMM (LoG) approach. Our algorithms can process dense tensors with any linear tensor layout, arbitrary tensor order and dimensions all of which can be runtime variable. We discuss different tensor slicing methods with parallelization strategies and propose six algorithm versions that call BLAS with subtensors or tensor slices. Their performance is quantified on a set of tensors with various shapes and tensor orders. Our best performing version attains a median performance of 1.37 double precision Tflops on an Intel Xeon Gold 6248R processor using Intel’s MKL. We show that the tensor layout does not affect the performance significantly. Our fastest implementation is on average at least 14.05% and up to 3.79x faster than other state-of-the-art approaches and actively developed libraries like Libtorch and Eigen.

1 Introduction

Tensor computations are found in many scientific fields such as computational neuroscience, pattern recognition, signal processing and data mining [5, 12]. These computations use basic tensor operations as building blocks for decomposing and analyzing multidimensional data which are represented by tensors [6, 7]. Tensor contractions are an important subset of basic operations that need to be fast for efficiently solving tensor methods.

There are three main approaches for implementing tensor contractions. The Transpose-Transpose-GEMM-Transpose (TTGT) approach reorganizes (flattens) tensors in order to perform a tensor contraction using optimized General Matrix Multiplication (GEMM) implementations [1, 14]. Implementations of the GEMM-like Tensor-Tensor multiplication (GETT) method have macro-kernels that are similar to the ones used in fast GEMM implementations [10, 15]. The third method is the Loops-over-GEMM (LoG) approach in which BLAS are utilized with multiple tensor slices or subtensors if possible [2, 8, 11, 13]. Implementations of the LoG and TTGT approaches are in general easier to maintain and faster to port than GETT implementations which might need to adapt vector instructions or blocking parameters according to a processor’s microarchitecture.

In this work, we present high-performance algorithms for the tensor-matrix multiplication which is used in many numerical methods such as the alternating least squares method [6, 7]. It is a compute-bound tensor operation and has the same arithmetic intensity as a matrix-matrix multiplication which can almost reach the practical peak performance of a computing machine.

To our best knowledge, we are the first to combine the LoG approach described in [2] with the findings on tensor slicing for the tensor-matrix multiplication in [8]. Our proposed algorithms support dense tensors with any order, dimensions and any linear tensor layout including the first- and the last-order storage formats for any contraction mode all of which can be runtime variable. They compute the tensor-matrix product in parallel using efficient GEMM or batched GEMM without transposing or flattening tensors. Despite their high performance, all algorithms are layout-oblivious and provide a sustained performance independent of the tensor layout without tuning.

Moreover, every proposed algorithm can be implemented with less than 150 lines of C++ code where the algorithmic complexity is reduced by the BLAS implementation and the corresponding selection of subtensors or tensor slices. We have provided an open and free reference C++ implementation of all algorithms and a python interface for convenience. While Intel’s MKL is used for our benchmarks, the user is free to select any other library that provides the BLAS interface.

The following analysis quantifies the impact of the tensor layout, the tensor slicing method and parallel execution of slice-matrix multiplications with varying contraction modes. The runtime measurements of our implementations are compared with state-of-the-art approaches discussed in [10, 15] and actively developed libraries including Libtorch and Eigen. In summary, the main findings of our work are:

- A tensor-matrix multiplication can be implemented by an in-place algorithm with 1 `gemv` and 7 `gemm` calls, supporting all combinations of contraction mode, tensor order and dimensions for any linear tensor layout.
- Our fastest algorithm is on average 17% faster than Intel’s `gemm_batch` when the contraction and leading dimensions of the tensors are greater than 256.
- The proposed algorithms are layout-oblivious. Their performance does not vary significantly for different tensor layouts if the contraction conditions remain the same.
- Our fastest algorithm computes the tensor-matrix multiplication on average, by at least 14.05% and up to a factor of 3.79 faster than other state-of-the-art library implementations, including LibTorch and Eigen.

The remainder of the paper is organized as follows. Section 2 presents related work. Section 3 introduces some notation on tensors and defines the tensor-matrix multiplication. Algorithm design and methods for slicing and parallel execution are discussed in Section 4. Section 5 describes the test setup. Benchmark results are presented in Section 6. Conclusions are drawn in Section 7.

83 2 Related Work

84 The authors of [15] present a tensor-contraction generator TCCG and the GETT
 85 approach for dense tensor contractions that is inspired from the design of a high-
 86 performance GEMM. Their unified code generator selects implementations from
 87 generated GETT, LoG and TTGT candidates. Their findings show that among
 88 48 different contractions 15% of LoG-based implementations are the fastest.

89 The author presents in [10] a runtime flexible tensor contraction library that
 90 uses GETT approach as well. He describes block-scatter-matrix algorithm which
 91 uses a special layout for the tensor contraction. The proposed algorithm yields
 92 results that feature a similar runtime behavior to those presented in [15].

93 The work in [8] introduces InTensLi, a framework that generates in-place
 94 tensor-matrix multiplication according to the LOG approach. The authors dis-
 95 cusses optimization and tuning techniques for slicing and parallelizing the op-
 96 eration. With optimized tuning parameters, they report a speedup of up to 4x
 97 over the TTGT-based MATLAB tensor toolbox library discussed in [1].

98 In [2], the author presents LoG-based algorithms that compute the tensor-
 99 vector product. They support dense tensors with linear tensor layouts, arbitrary
 100 dimensions and tensor order. The presented approach is to divide into eight cases
 101 calling GEMV and DOT. He reports average speedups of 6.1x and 4.0x compared
 102 to implementations that use the TTGT and GETT approach, respectively.

103 3 Background

104 **Notation** An order- p tensor is a p -dimensional array [9] where tensor ele-
 105 ments are contiguously stored in memory. We write a , \mathbf{a} , \mathbf{A} and $\underline{\mathbf{A}}$ in order
 106 to denote scalars, vectors, matrices and tensors. If not otherwise mentioned, we
 107 assume $\underline{\mathbf{A}}$ to have a tensor order that is greater than 2. The p -tuple \mathbf{n} with
 108 $\mathbf{n} = (n_1, n_2, \dots, n_p)$ will be referred to as a dimension tuple with $n_r > 1$. We
 109 will use round brackets $\underline{\mathbf{A}}(i_1, i_2, \dots, i_p)$ or $\underline{\mathbf{A}}(\mathbf{i})$ to denote a tensor element where
 110 $\mathbf{i} = (i_1, i_2, \dots, i_p)$ is a multi-index. A subtensor is denoted by $\underline{\mathbf{A}}'$ and references
 111 elements of a tensor $\underline{\mathbf{A}}$. They are specified with p index ranges and form a selec-
 112 tion grid. In this work, the index range shall either address all indices of a given
 113 mode or a single element that are given by single indices i_r with $1 \leq r \leq p$.
 114 Elements n'_r of a subtensor's dimension tuple \mathbf{n}' are therefore n_r if all indices
 115 of mode r are selected and 1 otherwise. We will annotate subtensors using only
 116 their non-unit modes such as $\underline{\mathbf{A}}'_{u,v,w}$ where $n_u > 1, n_v > 1$ and $n_w > 1$ and
 117 $1 \leq u \neq v \neq w \leq p$. It is sufficient to only provide non-unit modes as the
 118 remaining single indices correspond to the loop induction variables of the fol-
 119 lowing algorithms. A subtensor is called a slice $\underline{\mathbf{A}}'_{u,v}$ if the full range selection
 120 of $\underline{\mathbf{A}}$ occurs with only two modes. A fiber $\underline{\mathbf{A}}'_u$ is a tensor slice with only one
 121 dimension greater than 1.

122 **Linear Tensor Layouts** We use a layout tuple $\boldsymbol{\pi} \in \mathbb{N}^p$ to encode all linear ten-
 123 sor layouts including the first-order or last-order layout. They contain permuted

tensor modes whose priority is given by their index. The general k -order tensor layout for an order- p tensor is given by the layout tuple $\boldsymbol{\pi}$ with $\pi_r = k - r + 1$ for $1 < r \leq k$ and r for $k < r \leq p$. For instance, the first- and last-order storage formats are given by $\boldsymbol{\pi}_F = (1, 2, \dots, p)$ and $\boldsymbol{\pi}_L = (p, p-1, \dots, 1)$. An inverse layout tuple $\boldsymbol{\pi}^{-1}$ is defined by $\boldsymbol{\pi}^{-1}(\boldsymbol{\pi}(k)) = k$. Given a layout tuple $\boldsymbol{\pi}$ with p modes, the π_r -th element of a stride tuple is given by $w_{\pi_r} = \prod_{k=1}^{r-1} n_{\pi_k}$ for $1 < r \leq p$ and $w_{\pi_1} = 1$. Tensor elements of the π_1 -th mode are contiguously stored in memory. The location of tensor elements is determined by the tensor layout and the layout function. For a given tensor layout and stride tuple, a layout function $\lambda_{\mathbf{w}}$ maps a multi-index to a scalar index with $\lambda_{\mathbf{w}}(\mathbf{i}) = \sum_{r=1}^p w_r(i_r - 1)$.

Non-Modifying Flattening and Reshaping The flattening operation $\varphi_{r,q}$ transforms an order- p tensor $\underline{\mathbf{A}}$ to another order- p' view $\underline{\mathbf{B}}$ that has different a shape \mathbf{m} and layout $\boldsymbol{\tau}$ tuple of length p' with $p' = p - q + r$ and $1 \leq r < q \leq p$. It is related to the tensor unfolding operation as defined in [6, p.459] but neither changes the element ordering nor copies tensor elements. Given a layout tuple $\boldsymbol{\pi}$ of $\underline{\mathbf{A}}$, the flattening operation $\varphi_{r,q}$ is defined for contiguous modes $\hat{\boldsymbol{\pi}} = (\pi_r, \pi_{r+1}, \dots, \pi_q)$ of $\boldsymbol{\pi}$. Let $j = 0$ if $k \leq r$ and $j = q - r$ otherwise for $1 \leq k \leq p'$. Then the resulting layout tuple $\boldsymbol{\tau} = (\tau_1, \dots, \tau_{p'})$ of $\underline{\mathbf{B}}$ is given by $\tau_r = \min(\boldsymbol{\pi}_{r,q})$ and $\tau_k = \pi_{k+j} + s_k$ if $k \neq r$ where $s_k = |\{\pi_i \mid \pi_{k+j} > \pi_i \wedge \pi_i \neq \min(\hat{\boldsymbol{\pi}}) \wedge r \leq i \leq p\}|$. Elements of the shape tuple \mathbf{m} are defined by $m_{\tau_r} = \prod_{k=r}^q n_{\pi_k}$ and $m_{\tau_k} = n_{\pi_{k+j}}$ if $k \neq r$. Reshaping ρ transforms an order- p tensor $\underline{\mathbf{A}}$ to another order- p tensor $\underline{\mathbf{B}}$ with the shape tuple \mathbf{m} and layout tuple $\boldsymbol{\tau}$ tuples, both of length p . In this work, it permutes the shape and layout tuple simultaneously without changing the element ordering and without copying tensor elements. The operation ρ is defined by a permutation tuple $\boldsymbol{\rho} = (\rho_1, \dots, \rho_p)$ that defines elements of \mathbf{m} and $\boldsymbol{\tau}$ with $m_{\tau_r} = n_{\rho_r}$ and $\tau_r = \pi_{\rho_r}$, respectively.

Tensor-Matrix Multiplication Let $\underline{\mathbf{A}}$ and $\underline{\mathbf{C}}$ be order- p tensors with shapes $\mathbf{n}_a = (n_1, \dots, n_q, \dots, n_p)$ and $\mathbf{n}_c = (n_1, \dots, n_{q-1}, m, n_{q+1}, \dots, n_p)$. Let \mathbf{B} be a matrix of shape $\mathbf{n}_b = (m, n_q)$. A mode- q tensor-matrix product is denoted by $\underline{\mathbf{C}} = \underline{\mathbf{A}} \times_q \mathbf{B}$. An element of $\underline{\mathbf{C}}$ is defined by

$$\underline{\mathbf{C}}(i_1, \dots, i_{q-1}, j, i_{q+1}, \dots, i_p) = \sum_{i_q=1}^{n_q} \underline{\mathbf{A}}(i_1, \dots, i_q, \dots, i_p) \cdot \mathbf{B}(j, i_q) \quad (1)$$

with $1 \leq i_r \leq n_r$ and $1 \leq j \leq m$, see [6, 8]. Mode q is called the *contraction mode* with $1 \leq q \leq p$. The tensor-matrix multiplication generalizes the computational aspect of the two-dimensional case $\mathbf{C} = \mathbf{B} \cdot \mathbf{A}$ if $p = 2$ and $q = 1$. Its arithmetic intensity is equal to that of a matrix-matrix multiplication and is not memory-bound. In the following, we assume that the tensors $\underline{\mathbf{A}}$ and $\underline{\mathbf{C}}$ have the same tensor layout $\boldsymbol{\pi}$. Elements of matrix \mathbf{B} can be stored either in the column-major or row-major format. Without loss of generality, we assume $\underline{\mathbf{B}}$ to have the row-major storage format in this work. Also note that all of the following analysis is valid, if the matrix indices j and i_q are swapped.

164 4 Algorithm Design

165 4.1 Sequential Algorithm

166 The sequential baseline algorithm for Eq. 1 can be implemented with a single
 167 C++ function. It consists of nested recursion with a control flow that is akin to
 168 algorithm 1 in [3] consisting of two `if` statements with an `else` branch. The
 169 body of the first `if` statement contains a recursive call that skips the iteration
 170 over the dimension n_q when $r = \hat{q}$ with $\pi_r = q$ and $\hat{q} = \pi_q^{-1}$. The second `if`
 171 statement contains multiple recursive calls for the modes $1 \leq r \neq \hat{q} \leq p$ with
 172 different multi-indices. The `else` branch is the base case and consists of two
 173 loops that compute a fiber-matrix product. The outer loop iterates with j over
 174 the dimension m of $\underline{\mathbf{C}}$ and \mathbf{B} . The inner loop iterates with i_q over the dimension
 175 n_q of $\underline{\mathbf{A}}$ and \mathbf{B} computing an inner product.

176 4.2 Baseline Algorithm with Contiguous Memory Access

177 The baseline algorithm improves the sequential version and accesses elements of
 178 $\underline{\mathbf{A}}$ and $\underline{\mathbf{C}}$ non-contiguously whenever $\pi_1 \neq q$. Matrix \mathbf{B} is contiguously accessed
 179 if i_q or j is incremented with unit-strides depending on the storage format of $\underline{\mathbf{B}}$.
 180 The access pattern can be improved by reordering tensor elements according to
 181 the storage format. However, copy operations reduce the overall throughput of
 182 the operation [13].

183 A better way is to access tensor elements according to the tensor layout with
 184 the help of the tensor layout tuple π as proposed in [3]. The modified Algorithm 1
 185 contiguously accesses memory for $\pi_1 \neq q$ and $p > 1$. Each recursion level adjusts
 186 only one multi-index element i_{π_r} with a stride w_{π_r} in line 5. With increasing
 187 recursion level and decreasing r , indices are incremented with smaller strides as
 188 $w_{\pi_r} \leq w_{\pi_{r+1}}$. The condition of the second `if` statement in line 4 is changed from
 189 $r \geq 1$ to $r > 1$. In this way, the mode- π_1 loop with index i_{π_1} and the minimum
 190 stride w_{π_1} are included in the base case which contains three loops performing
 191 a slice-matrix multiplication. The loop ordering are adjusted according to the
 192 tensor and matrix layout. The inner-most loop increments i_{π_1} and contiguously
 193 accesses tensor elements of $\underline{\mathbf{A}}$ and $\underline{\mathbf{C}}$. The second loop increments i_q with which
 194 elements of \mathbf{B} are contiguously accessed if \mathbf{B} is stored in the row-major format.
 195 The third loop increments j and could be placed as the second loop if \mathbf{B} is stored
 196 in the column-major format.

197 While spatial data locality is improved by adjusting the loop ordering, the
 198 temporal data locality of tensors $\underline{\mathbf{A}}$ and $\underline{\mathbf{C}}$ differ. Note that slice $\underline{\mathbf{A}}'_{\pi_1, q}$, fiber $\underline{\mathbf{C}}'_{\pi_1}$
 199 and element $\underline{\mathbf{B}}(j, i_q)$ are accessed m , n_q and n_{π_1} times, respectively. While the
 200 specified fiber of $\underline{\mathbf{C}}$ can fit into first or second level cache, slice elements of $\underline{\mathbf{A}}$
 201 are unlikely to fit in the local caches if the slice size $n_{\pi_1} \times n_q$ is large leading to
 202 higher cache misses and suboptimal performance. Instead of optimizing for better
 203 temporal data locality, we use existing high-performance BLAS implementations
 204 for the base case.

```

1 tensor_times_matrix(A, B, C, n, i, m, q, q̂, r)
2   if  $r = \hat{q}$  then
3     | tensor_times_matrix(A, B, C, n, i, m, q, q̂,  $r - 1$ )
4   else if  $r > 1$  then
5     | for  $i_{\pi_r} \leftarrow 1$  to  $n_{\pi_r}$  do
6       | | tensor_times_matrix(A, B, C, n, i, m, q, q̂,  $r - 1$ )
7   else
8     | for  $j \leftarrow 1$  to  $m$  do
9       | | for  $i_q \leftarrow 1$  to  $n_q$  do
10        | | | for  $i_{\pi_1} \leftarrow 1$  to  $n_{\pi_1}$  do
11        | | | | C( $i_1, \dots, i_{q-1}, j, i_{q+1}, \dots, i_p$ ) += A( $i_1, \dots, i_q, \dots, i_p$ ) · B( $j, i_q$ )

```

Algorithm 1: Modified baseline algorithm with contiguous memory access for the tensor-matrix multiplication. The tensor order must be greater than one and for the contraction mode $1 \leq q \leq p$ and $\pi_1 \neq q$ must hold. The algorithm needs to be initially called with $r = p$ where \mathbf{n} is the shape tuple of $\underline{\mathbf{A}}$ and m is the q -th dimension of $\underline{\mathbf{C}}$.

205 4.3 BLAS-based Algorithms with Tensor Slices

206 Algorithm 1 is the starting point for the BLAS-based algorithm which computes
 207 the tensor-matrix product with a `gemm` routine. Besides the illustrated algorithm,
 208 we have identified seven other cases where a single `gemm` call suffices to compute
 209 the tensor-matrix product even if the tensor order $p > 2$. In summary, there
 210 are eight cases with a single `gemm` call using different arguments which are listed
 211 in table 1. The list of `gemm` calls supports all linear tensor layout and has no
 212 limitation on tensor order and contraction mode. The arguments of `gemm` are
 213 chosen depending on the tensor order p , tensor layout π and contraction mode
 214 q except for the `CBLAS_ORDER` which is `CblasRowMajor`. The following description
 215 can be used to also define eight cases for the `CblasColMajor` format. You can find
 216 the parameter arguments in our C++ library.

217 *Case 1* ($p = 1$): The tensor-vector product $\underline{\mathbf{A}} \times_1 \mathbf{B}$ can be computed with a
 218 `gemv` operation $\mathbf{a}^T \cdot \mathbf{B}$ where $\underline{\mathbf{A}}$ is an order-1 tensor, i.e. a vector \mathbf{a} of length n_1 .

219 *Case 2-5* ($p = 2$): If $\underline{\mathbf{A}}$ and $\underline{\mathbf{C}}$ are order-2 tensors, i.e. a matrix \mathbf{A} with
 220 dimensions n_1 and n_2 , then a single `gemm` suffices to compute the tensor-matrix
 221 product. If \mathbf{A} and \mathbf{C} have the column-major format with $\pi = (1, 2)$, `gemm` either
 222 executes $\mathbf{C} = \mathbf{A} \cdot \mathbf{B}^T$ for $q = 1$ or $\mathbf{C} = \mathbf{B} \cdot \mathbf{A}$ for $q = 2$. Note that `gemm` interprets
 223 \mathbf{C} and \mathbf{A} as matrices using the reshaping operation ρ with $\rho = (2, 1)$ in row-
 224 major format even though both are stored column-wise. If \mathbf{A} and \mathbf{C} have the
 225 row-major format with $\pi = (2, 1)$, `gemm` either executes $\mathbf{C} = \mathbf{B} \cdot \mathbf{A}$ for $q = 1$ or
 226 $\mathbf{C} = \mathbf{A} \cdot \mathbf{B}^T$ for $q = 2$. The transposition of \mathbf{B} is necessary for the cases 2,5 and
 227 independent of the chosen storage format.

228 *Case 6-7* ($p > 2$): If the order of $\underline{\mathbf{A}}$ and $\underline{\mathbf{C}}$ is greater than 2 and if the
 229 contraction mode q is equal to π_1 (case 6), a single `gemm` with the depicted

| Case | Order p | Layout π | Mode q | Routine | T | M | N | K | A | LDA | B | LDB | LDC |
|------|-----------|--------------|---------------------------|--------------|----------|-------------|-------------|-------|-----------------|-------|-----------------|-------------|-------------|
| 1 | 1 | - | 1 | gemv | - | m | n_1 | - | B | n_1 | <u>A</u> | - | - |
| 2 | 2 | (1, 2) | 1 | gemm | B | n_2 | m | n_1 | <u>A</u> | n_1 | B | n_1 | m |
| 3 | 2 | (1, 2) | 2 | gemm | - | m | n_1 | n_2 | B | n_2 | <u>A</u> | n_1 | n_1 |
| 4 | 2 | (2, 1) | 1 | gemm | - | m | n_2 | n_1 | B | n_1 | <u>A</u> | n_2 | n_2 |
| 5 | 2 | (2, 1) | 2 | gemm | B | n_1 | m | n_2 | <u>A</u> | n_2 | B | n_2 | m |
| 6 | > 2 | any | π_1 | gemm | B | \bar{n}_q | m | n_q | <u>A</u> | n_q | B | n_q | m |
| 7 | > 2 | any | π_p | gemm | - | m | \bar{n}_q | n_q | B | n_q | <u>A</u> | \bar{n}_q | \bar{n}_q |
| 8 | > 2 | any | π_2, \dots, π_{p-1} | gemm* | - | m | n_{π_1} | n_q | B | n_q | <u>A</u> | w_q | w_q |

Table 1. Eight cases with **gemv** and **gemm** for the mode- q tensor-matrix multiplication. Arguments T, M, N, etc. of the BLAS are chosen with respect to the tensor order p , layout π and contraction mode q where T specifies if **B** is transposed. **gemm*** denotes multiple **gemm** calls with different tensor slices. Argument \bar{n}_q for case 6 and 7 is given by $\bar{n}_q = 1/n_q \prod_r^p n_r$. Matrix **B** has the row-major format.

arguments executes $\mathbf{C} = \mathbf{A} \cdot \mathbf{B}^T$ and computes a tensor-matrix product $\underline{\mathbf{C}} = \underline{\mathbf{A}} \times_{\pi_1} \mathbf{B}$ for any storage layout of **A** and **C**. Tensors **A** and **C** are flattened with $\varphi_{2,p}$ to row-major matrices **A** and **C**. Matrix **A** has $\bar{n}_{\pi_1} = \bar{n}/n_{\pi_1}$ rows and n_{π_1} columns while matrix **C** has the same number of rows and m columns. If $\pi_p = q$ (case 7), Tensors **A** and **C** are flattened with $\varphi_{1,p-1}$ to column-major matrices **A** and **C**. Matrix **A** has n_{π_p} rows and $\bar{n}_{\pi_p} = \bar{n}/n_{\pi_p}$ columns while matrix **C** has m rows and the same number of columns. A single **gemm** executes $\mathbf{C} = \mathbf{B} \cdot \mathbf{A}$ and computes the tensor-matrix product $\underline{\mathbf{C}} = \underline{\mathbf{A}} \times_{\pi_p} \mathbf{B}$ for any storage layout of **A** and **C**. Note that in all cases no copy operation is performed in order to compute the desired contraction, see subsection 3.

Case 8 ($p > 2$): If the tensor order is greater than 2 with $\pi_1 \neq q$ and $\pi_p \neq q$, the modified baseline algorithm 1 is used to successively call $\bar{n}/(n_q \cdot n_{\pi_1})$ times **gemm** with different tensor slices of **C** and **A**. Each **gemm** computes one slice $\underline{\mathbf{C}}'_{\pi_1,q}$ of the tensor-matrix product **C** using the corresponding tensor slices **A**' $_{\pi_1,q}$ and the matrix **B**. The matrix-matrix product $\mathbf{C} = \mathbf{B} \cdot \mathbf{A}$ is performed by interpreting both tensor slices as row-major matrices **A** and **C** which have the dimensions (n_q, n_{π_1}) and (m, n_{π_1}) , respectively. Please note that Algorithm 2 in [8] suggests to transpose matrix **B**.

4.4 BLAS-Based Algorithms with Subtensors

Case 8 can be optimized by utilizing larger subtensors instead of tensor slices. This can be accomplished by adding mergeable modes to the slice-matrix multiplication in which the subtensor can be flattened into a matrix without reordering tensor elements, see lemma 4.1 in [8]. We will use our flattening operation which does not copy or reorder elements, see section 3. The number of mergeable modes is $\hat{q}-1$ with $\hat{q} = \pi^{-1}(q)$ and the corresponding modes are $\pi_1, \pi_2, \dots, \pi_{\hat{q}-1}$. Applying flattening $\varphi_{1,q-1}$ and reshaping ρ with $\rho = (2, 1)$ on a subtensor of

$\underline{\mathbf{A}}$ with dimensions $n_{\pi_1}, \dots, n_{\pi_{\hat{q}-1}}, n_q$ yields a row-major matrix \mathbf{A} with shape $(n_q, \prod_{r=1}^{\hat{q}-1} n_{\pi_r})$. Analogously, tensor $\underline{\mathbf{C}}$ becomes a row-major matrix with the shape $(m, \prod_{r=1}^{\hat{q}-1} n_{\pi_r})$. This description supports all linear tensor layouts and generalizes lemma 4.2 in [8].

Algorithm 1 needs a minor modification so that `gemm` can be used with flattened subtensors instead of tensor slices. The modified algorithm therefor iterates only over modes larger than \hat{q} in the non-base case and hence omits the first \hat{q} modes $\pi_{1,\hat{q}} = (\pi_1, \dots, \pi_{\hat{q}})$ with $\pi_{\hat{q}} = q$. The conditions in line 2 and 4 are changed to $1 < r \leq \hat{q}$ and $\hat{q} < r$, respectively. The single indices of the subtensors $\underline{\mathbf{A}}'_{\pi_{1,\hat{q}}}$ and $\underline{\mathbf{C}}'_{\pi_{1,\hat{q}}}$ are given by the loop induction variables that belong to the π_r -th loop with $\hat{q} + 1 \leq r \leq p$.

4.5 Parallel BLAS-based Algorithms

The following paragraphs discuss three parallel approaches for the eighth case. Cases 1 to 7 already call a multi-threaded `gemm`.

Sequential Loops and Multithreaded Matrix Multiplication A simple approach is to leave algorithm 1 unmodified and sequentially call a multi-threaded `gemm` in the base case as described in subsection 4.3. This is beneficial if $q = \pi_{p-1}$, if the inner dimensions n_{π_1}, \dots, n_q are large or if the outer-most dimension n_{π_p} is smaller than the available processor cores. However, if the above conditions are not met, the processor cores might not be fully utilized where each multi-threaded `gemm` is executed with small subtensors. We will refer to this algorithm version as `<seq-loops,par-gemm>` that is executable with subtensors or tensor slices.

Parallel Loops and Single or Multithreaded Matrix Multiplication A more advanced version of the above algorithm executes a single-threaded `gemm` in parallel with all available (free) modes. The number of free modes depends on the tensor slicing. If subtensors are used, all $\pi_{\hat{q}+1}, \dots, \pi_p$ modes are free and can be used for parallel execution. In case of tensor slices, only π_1 and $\pi_{\hat{q}}$ are free modes. The corresponding maximum degree of parallelism for both cases is $\prod_{r=\hat{q}+1}^p n_{\pi_r}$ and $\prod_{r=1}^p n_r / (n_{\pi_1} n_{\pi_{\hat{q}}})$, respectively.

Using tensor slices for the multiplication, $\underline{\mathbf{A}}$ and $\underline{\mathbf{C}}$ are flattened twice with $\varphi_{\pi_{\hat{q}+1}, \pi_p}$ and $\varphi_{\pi_2, \pi_{\hat{q}-1}}$. The resulting tensor is of order 4 with dimensions $n_{\pi_1}, \hat{n}_{\pi_2}, n_q, \hat{n}_{\pi_4}$ where $\hat{n}_{\pi_2} = \prod_{r=2}^{\hat{q}-1} n_{\pi_r}$ and $\hat{n}_{\pi_4} = \prod_{r=\hat{q}+1}^p n_{\pi_r}$. In this way the tree-recursion has been transformed in two loops. The outer loop iterates over \hat{n}_{π_4} while the inner loop iterates over \hat{n}_{π_2} calling `gemm` with slices $\underline{\mathbf{A}}'_{\pi_1, q}$ and $\underline{\mathbf{C}}'_{\pi_1, q}$. Both loops are parallelized using `omp parallel for` together with the `collapse(2)` and the `num_threads` clause which specifies the thread number.

In case of the general subtensor-matrix approach, both tensors are flattened twice with $\varphi_{\pi_{\hat{q}+1}, \pi_p}$ and $\varphi_{\pi_1, \pi_{\hat{q}-1}}$. The resulting tensor is of order 3 with dimensions $\hat{n}_{\pi_1}, n_q, \hat{n}_{\pi_4}$ where $\hat{n}_{\pi_1} = \prod_{r=1}^{\hat{q}-1} n_{\pi_r}$ and $\hat{n}_{\pi_4} = \prod_{r=\hat{q}+1}^p n_{\pi_r}$. The corresponding algorithm consists of one loops which iterates over \hat{n}_{π_4} calling single-threaded `gemm` with multiple subtensors $\underline{\mathbf{A}}'_{\pi', q}$ and $\underline{\mathbf{C}}'_{\pi', q}$ with $\pi' = (\pi_1, \dots, \pi_{\hat{q}-1})$.

Both algorithm variants will be referred to as `<par-loops,seq-gemm>` which can be used with subtensors or tensor slices. Note that `<seq-loops,par-gemm>` and `<par-loops,seq-gemm>` are opposing versions where either `gemm` or the free loops are performed in parallel. The all-parallel version `<par-loops,par-gemm>` executes available loops in parallel where each loop thread executes a multi-threaded `gemm` with either subtensors or tensor slices.

Multithreaded batched Matrix Multiplication The next version of the base algorithm is a modified version of the general subtensor-matrix approach that calls a single batched `gemm` for the eighth case. The subtensor dimensions and remaining `gemm` arguments remain the same. The library implementation is responsible how subtensor-matrix multiplications are executed and if subtensors are further divided into smaller subtensors or tensor slices. This version will be referred to as the `<gemm_batch>` variant.

5 Experimental Setup

Computing System The experiments have been carried out on an Intel Xeon Gold 6248R processor with a Cascade micro-architecture. The processor consists of 24 cores operating at a base frequency of 3 GHz. With 24 cores and a peak AVX-512 boost frequency of 2.5 GHz, the processor achieves a theoretical data throughput of ca. 1.92 double precision Tflops. We measured a peak performance of 1.78 double precision Tflops using the likwid performance tool.

We have used the GNU compiler v10.2 with the highest optimization level `-O3` and `-march=native`, `-pthread` and `-fopenmp`. Loops within for the eighth case have been parallelized using GCC’s OpenMP v4.5 implementation. We have used the `gemv` and `gemm` implementation of the 2024.0 Intel MKL and its own threading library `mk1_intel_thread` together with the threading runtime library `libiomp5`.

If not otherwise mentioned, both tensors $\underline{\mathbf{A}}$ and $\underline{\mathbf{C}}$ are stored according to the first-order linear tensor layout with $\pi = (1, \dots, p)$ whereas matrix \mathbf{B} has the row-major storage format.

Tensor Shapes We have used asymmetrically and symmetrically shaped tensors in order to cover many use cases. The dimension tuples of both shape types are organized within two three-dimensional arrays with which tensors are initialized. The dimension array for the first shape type contains $720 = 9 \times 8 \times 10$ dimension tuples where the row number is the tensor order ranging from 2 to 10. For each tensor order, 8 tensor instances with increasing tensor size is generated. A special feature of this test set is that the contraction dimension and the leading dimension are disproportionately large. The second set consists of $336 = 6 \times 8 \times 7$ dimensions tuples where the tensor order ranges from 2 to 7 and has 8 dimension tuples for each order. Each tensor dimension within the second set is 2^{12} , 2^8 , 2^6 , 2^5 , 2^4 and 2^3 . A detailed explanation of the tensor shape setup is given in [2, 3].

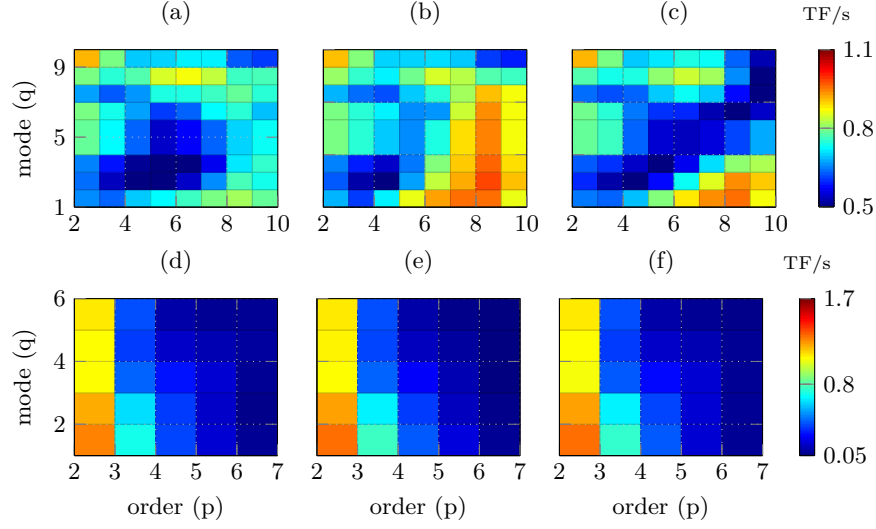


Fig. 1. Performance maps in double-precision Tflops of the proposed algorithms with varying tensor orders p and contraction modes q . Tensors are asymmetrically shaped on the top plots and symmetrically shaped on the bottom plots. In (a) and (d) function `<gemm_batch>` is executed, in (b) and (e) `<par-loops,seq-gemm>` with tensor slices, in (c) and (f) `<par-loops,seq-gemm>` with subtensors.

6 Results and Discussion

Slicing Methods The next paragraphs analyze the two proposed slicing methods and discuss runtime results of `<par-loops,seq-gemm>` and `<gemm_batch>` using asymmetrically and symmetrically shaped tensors. Fig. 1 contains six contour plots (performance maps) in which `<par-loops,seq-gemm>` either uses subtensors or tensor slices and `<gemm_batch>` loops over subtensors only. Each point within the performance map represents a mean value that has been averaged over tensor sizes for a tensor order¹.

For asymmetrically shaped tensors, function `<par-loops,seq-gemm>` with tensor slices performs on average 18% better than with subtensors and is on average 11% faster than Intel’s `gemm_batch` routine. It reaches almost 1.1 Tflops for non-edge cases with $q > 2$ and $p > 6$. This suggests that the Intel’s implementation does not divide subtensors into smaller blocks.

With symmetrically shaped tensors, `<par-loops,seq-gemm>` with tensor slices and `<gemm_batch>` perform almost equally well and reach 221.52 Gflops and 236.21 Gflops, respectively. Moreover, the slicing method seems to have only little affect on the overall runtime behavior of `<par-loops,seq-gemm>`. In contrast to the performance maps with asymmetrically shaped tensors, all functions al-

¹ Note that Fig. 2 suggests that the contraction mode q can be greater than p which is not possible. Our profiling program sets $q = p$ in such cases.

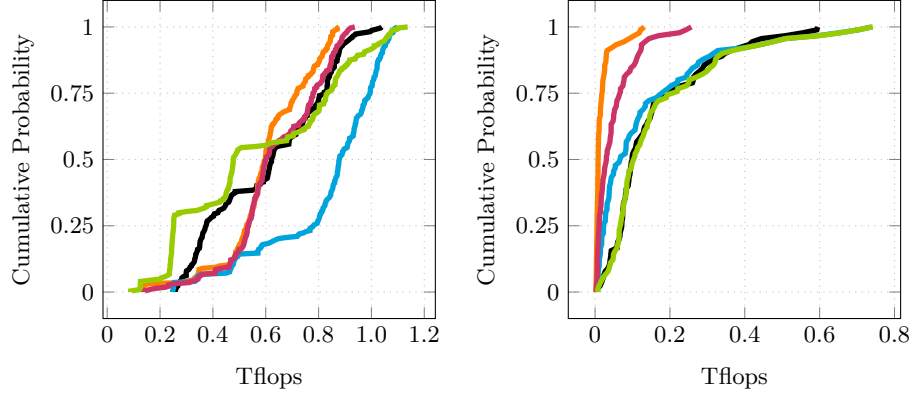


Fig. 2. Cumulative performance distributions of the proposed algorithms for the eighth case. Each distribution line belongs to one algorithm: `<gemm_batch>` (black), `<seq-loops,par-gemm>` (orange) and `<par-loops,seq-gemm>` (blue) using tensor slices, `<seq-loops,par-gemm>` (pink) and `<par-loops,seq-gemm>` (green) using subtenors. Tensors are asymmetrically (left plot) and symmetrically shaped (right plot).

most reach the attainable peak performance of 1.7 Tflops when $p = 2$. This can be by the fact that both dimensions are equal or larger than 4096 enabling `gemm` to operate under optimal conditions.

Parallelization Methods The contour plots in Fig. 1 contain performance data of all cases except for 4 and 5, see Table 1. The effects of the presented slicing and parallelization methods can be better understood if performance data of only the eighth case is examined. Fig. 2 contains cumulative performance distributions of all the proposed algorithms which are generated `gemm` or `gemm_batch` calls within case 8. As the distribution is empirically computed, the probability y of a point (x, y) on a distribution function corresponds to the number of test cases of a particular algorithm that achieves x or less Tflops. For instance, function `<seq-loops,par-gemm>` with subtenors computes the tensor-matrix product for 50% percent of the test cases with equal to or less than 0.6 Tflops in case of asymmetrically shaped tensor. Consequently, distribution functions with an exponential growth are favorable while logarithmic behavior is less desirable. The test set cardinality for case 8 is 255 for asymmetrically shaped tensors and 91 for symmetrically ones.

In case of asymmetrically shaped tensors, `<par-loops,seq-gemm>` with tensor slices performs best and outperforms `<gemm_batch>`. One unexpected finding is that function `<seq-loops,par-gemm>` with any slicing strategy performs better than `<gemm_batch>` when the tensor order p and contraction mode q satisfy $4 \leq p \leq 7$ and $2 \leq q \leq 4$, respectively. Functions executed with symmetrically shaped tensors reach at most 743 Gflops for the eighth case which is less than half of the attainable peak performance of 1.7 Tflops. This is expected as cases 2 and 3 are not considered. Functions `<par-loops,seq-gemm>` with subtenors

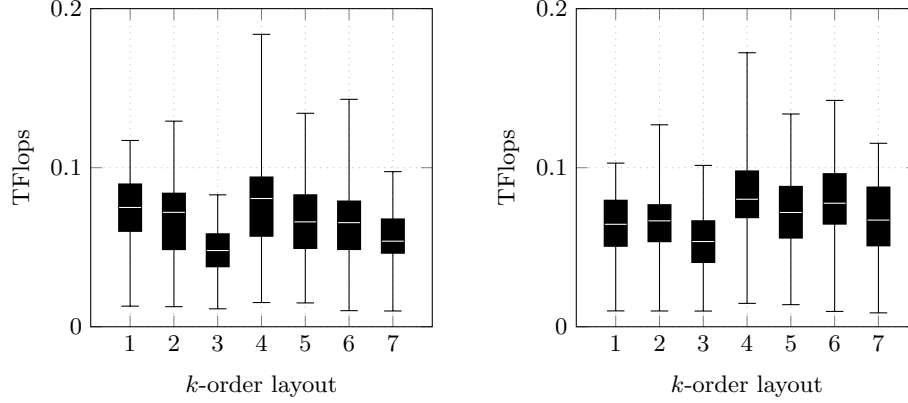


Fig. 3. Box plots visualizing performance statics in double-precision Tflops of `<gemm_batch>` (left) and `<par-loops, seq-gemm>` with subtensors (right). Box plot number k denotes the k -order tensor layout of symmetrically shaped tensors with order 7.

and `<gemm_batch>` have almost the same performance distribution outperforming `<seq-loops, par-gemm>` for almost every test case. Function `<par-loops, seq-gemm>` with tensor slices is on average almost as fast as with subtensors. However, if the tensor order is greater than 3 and the tensor dimensions are less than 64, its running time increases by almost a factor of 2.

These observations suggest to use `<par-loops, seq-gemm>` with tensor slices for common cases in which the leading and contraction dimensions are larger than 64 elements. Subtensors should only be used if the leading dimension n_{π_1} of $\underline{\mathbf{A}}_{\pi_1, q}$ and $\underline{\mathbf{C}}_{\pi_1, q}$ falls below 64. This strategy is different to the one presented in [8] that maximizes the number of modes involved in the matrix multiply. We have also observed no performance improvement if `par-gemm` was used with `par-loops` which is why their distribution functions are not shown in Fig. 2. Moreover, in most cases the `seq-loops` implementations are independent of the tensor shape slower than `par-loops`, even for smaller tensor slices.

Layout-Oblivious Algorithms Fig. 3 contains two subfigures visualizing performance statics in double-precision Tflops of `<gemm_batch>` (left subfigure) and `<par-loops, seq-gemm>` with subtensors (right subfigure). Each box plot with the number k has been computed from benchmark data with symmetrically shaped order-7 tensors with the k -order tensor layout. The 1-order and 7-order layout, for instance, are the first- and last-order storage formats for the order-7 tensor with $\pi_F = (1, 2, \dots, 7)$ and $\pi_L = (7, 6, \dots, 1)$. The definition of k -order tensor layouts can be found in section 3.

The low performance of around 70 Gflops can be attributed to the fact that the contraction dimension of subtensors of tensor slices of symmetrically shaped order-7 tensors are 8 while the leading dimension is 8 or at most 48 for subtensors. The relative standard deviation of `<gemm_batch>`'s and `<par-loops, seq-gemm>`'s

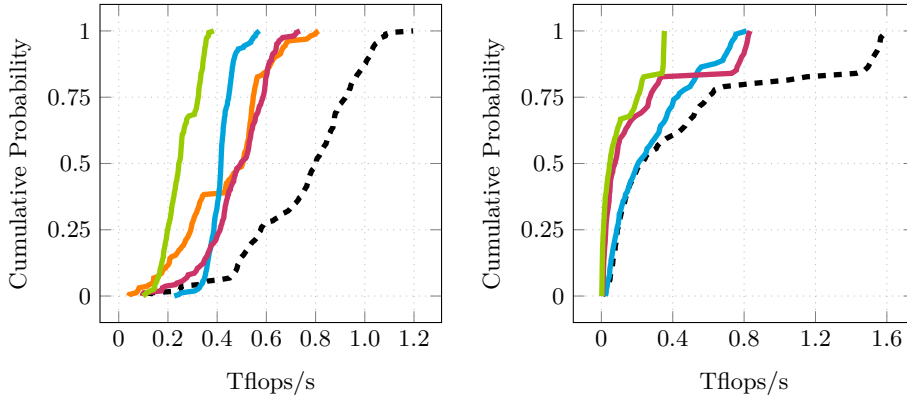


Fig. 4. Cumulative performance distributions of tensor-times-matrix algorithms in double-precision Tflops. Each distribution line belongs to a library: **tlib**[ours] (---), **tcl** (—), **tblis** (—), **libtorch** (—), **eigen** (—). Libraries have been tested with asymmetrically-shaped (left plot) and symmetrically-shaped tensors (right plot).

median values are 12.95% and 17.61%. Their respective interquartile range are similar with a relative standard deviation of 22.25% and 15.23%.

The runtime results with different k -order tensor layouts show that the performance of our proposed algorithms is not designed for a specific tensor layout. Moreover, the performance stays within an acceptable range independent of the tensor layout.

Comparison with other Approaches We have compared our best implementation with four libraries that implement the tensor-matrix multiplication using different approaches. Library **tcl** implements the TTGT approach with a high-perform tensor-transpose library **hptt** which is discussed in [15]. **tblis** implements the GETT approach that is akin to Blis’ algorithm design for the matrix multiplication [10]. The tensor extension of **eigen** (v3.3.7) is used by the Tensorflow framework. Library **libtorch** (v2.3.0) is the C++ distribution of PyTorch. **tlib** denotes our library using algorithm `<par-loops,seq-gemm>` that have been presented in the previous paragraphs.

Fig. 2 contains cumulative performance distributions for the complete test sets comparing the performance distribution of our implementation with the previously mentioned libraries. Note that we only have used tensor slices for asymmetrically shaped tensors (left plot) and subtensors for symmetrically shaped tensors (right plot). Our implementation with a median performance of 793.75 Gflops outperforms others’ for almost every asymmetrically shaped tensor in the test set. The median performances of **tcl**, **tblis**, **libtorch** and **eigen** are 503.61, 415.33, 496.22 and 244.69 Gflops reaching on average 74.11%, 61.14%, 76.68% and 39.34% of **tlib**’s throughputs.

In case of symmetrically shaped tensors the performance distributions of all libraries on the right plot in Fig. 2 are much closer. The median performances of

433 **tlib**, **tblis**, **libtorch** and **eigen** are 228.93, 208.69, 76.46, 46.25 Gflops reaching
 434 on average 73.06%, 38.89%, 19.79% of **tlib**'s throughputs². All libraries operate
 435 with 801.68 or less Gflops for the cases 2 and 3 which is almost half of **tlib**'s
 436 performance with 1579 Gflops. The median performance and the interquartile
 437 range of **tblis** and **tlib** for the cases 6 and 7 are almost the same. Their respective
 438 median Gflops are 255.23 and 263.94 for the sixth case and 121.17 and 144.27
 439 for the seventh case. This explains the similar performance distributions when
 440 their performance is less than 400 Gflops. **Libtorch** and **eigen** compute the
 441 tensor-matrix product, in median, with 17.11 and 9.64 Gflops/s, respectively.
 442 Our library **tlib** has a median performance of 102.11 Gflops and outperforms
 443 **tblis** with 79.35 Gflops for the eighth case.

444 7 Conclusion and Future Work

445 We presented efficient layout-oblivious algorithms for the compute-bound tensor-
 446 matrix multiplication which is essential for many tensor methods. Our approach
 447 is based on the LOG-method and computes the tensor-matrix product in-place
 448 without transposing tensors. It applies the flexible approach described in [2]
 449 and generalizes the findings on tensor slicing in [8] for linear tensor layouts.
 450 The resulting algorithms are able to process dense tensors with arbitrary tensor
 451 order, dimensions and with any linear tensor layout all of which can be runtime
 452 variable.

453 Our benchmarks show that dividing the base algorithm into eight different
 454 GEMM cases improves the overall performance. We have demonstrated that al-
 455 gorithms with parallel loops over single-threaded GEMM calls with tensor slices
 456 and subtensors perform best. Interestingly, they outperform a single batched
 457 GEMM with subtensors, on average, by 14% in case of asymmetrically shaped
 458 tensors and if tensor slices are used. Both version computes the tensor-matrix
 459 product on average faster than other state-of-the-art implementations. We have
 460 shown that our algorithms are layout-oblivious and do not need further refine-
 461 ment if the tensor layout is changed. We measured a relative standard deviation
 462 of 12.95% and 17.61% with symmetrically-shaped tensors for different k -order
 463 tensor layouts.

464 One can conclude that LOG-based tensor-times-matrix algorithms are on
 465 par or can even outperform TTGT-based and GETT-based implementations
 466 without losing their flexibility. Hence, other actively developed libraries such as
 467 LibTorch and Eigen might benefit from implementing the proposed algorithms.
 468 Our header-only library provides C++ interfaces and a python module which
 469 allows frameworks to easily integrate our library.

470 In the future, we intend to generalize LOG-based approach for general ten-
 471 sor contractions with the same flexibility that we offered for the tensor-matrix
 472 multiplication. We would like to further optimize the tensor-matrix multiplica-

² We were unable to run tcl with our test set containing symmetrically shaped tensors.
 We suspect a very high memory demand to be the reason.

tion based on benchmark results of matrix-matrix products which might lead to better runtime results for edge cases.

Source Code Availability Project description and source code can be found at <https://github.com/bassoy/ttm>. The sequential tensor-matrix multiplication of TLIB is part of uBLAS and in the official release of **Boost v1.70.0** and later.

References

1. Bader, B.W., Kolda, T.G.: Algorithm 862: Matlab tensor classes for fast algorithm prototyping. *ACM Trans. Math. Softw.* **32**, 635–653 (December 2006)
2. Bassoy, C.: Design of a high-performance tensor-vector multiplication with blas. In: *International Conference on Computational Science*. pp. 32–45. Springer (2019)
3. Bassoy, C., Schatz, V.: Fast higher-order functions for tensor calculus with tensors and subtensors. In: *International Conference on Computational Science*. pp. 639–652. Springer (2018)
4. Goto, K., Geijn, R.A.v.d.: Anatomy of high-performance matrix multiplication. *ACM Transactions on Mathematical Software (TOMS)* **34**(3) (2008)
5. Karahan, E., Rojas-López, P.A., Bringas-Vega, M.L., Valdés-Hernández, P.A., Valdes-Sosa, P.A.: Tensor analysis and fusion of multimodal brain images. *Proceedings of the IEEE* **103**(9), 1531–1559 (2015)
6. Kolda, T.G., Bader, B.W.: Tensor decompositions and applications. *SIAM review* **51**(3), 455–500 (2009)
7. Lee, N., Cichocki, A.: Fundamental tensor operations for large-scale data analysis using tensor network formats. *Multidimensional Systems and Signal Processing* **29**(3), 921–960 (2018)
8. Li, J., Battaglino, C., Perros, I., Sun, J., Vuduc, R.: An input-adaptive and in-place approach to dense tensor-times-matrix multiply. In: *High Performance Computing, Networking, Storage and Analysis*, 2015. pp. 1–12. IEEE (2015)
9. Lim, L.H.: Tensors and hypermatrices. In: Hogben, L. (ed.) *Handbook of Linear Algebra*. Chapman and Hall, 2 edn. (2017)
10. Matthews, D.A.: High-performance tensor contraction without transposition. *SIAM Journal on Scientific Computing* **40**(1), C1–C24 (2018)
11. Napoli, E.D., Fabregat-Traver, D., Quintana-Ortí, G., Bientinesi, P.: Towards an efficient use of the blas library for multilinear tensor contractions. *Applied Mathematics and Computation* **235**, 454 – 468 (2014)
12. Papalexakis, E.E., Faloutsos, C., Sidiropoulos, N.D.: Tensors for data mining and data fusion: Models, applications, and scalable algorithms. *ACM Transactions on Intelligent Systems and Technology (TIST)* **8**(2), 16 (2017)
13. Shi, Y., Niranjana, U.N., Anandkumar, A., Cecka, C.: Tensor contractions with extended blas kernels on cpu and gpu. In: *2016 IEEE 23rd International Conference on High Performance Computing (HiPC)*. pp. 193–202 (Dec 2016)
14. Solomonik, E., Matthews, D., Hammond, J., Demmel, J.: Cyclops tensor framework: Reducing communication and eliminating load imbalance in massively parallel contractions. In: *Parallel & Distributed Processing (IPDPS)*, 2013 IEEE 27th International Symposium on. pp. 813–824. IEEE (2013)
15. Springer, P., Bientinesi, P.: Design of a high-performance gemm-like tensor-tensor multiplication. *ACM Transactions on Mathematical Software (TOMS)* **44**(3), 28 (2018)